WATER RESOURCES RESEARCH, VOL. 35, NO. 5, PAGES 1471–1479, MAY 1999

Head and flux variability in heterogeneous unsaturated soils under transient flow conditions

Marco Ferrante
Istituto di Idraulica, Universita' degli Studi di Perugia, Perugia, Italy

T.-C. Jim Yeh
Department of Hydrology and Water Resources, University of Arizona, Tucson

Abstract. A numerical model for the analysis of uncertainty propagation in flow through unsaturated soils is developed. This model is based on a first-order Taylor series expansion of the discretized Richards equation. Soil hydrologic properties (the saturated hydraulic conductivity and the pore size distribution parameter) are assumed to be stochastic processes in space. The surface boundary conditions can be considered as deterministic variables in time or stochastic time series. Spectral analysis and Monte Carlo simulations were used to verify this numerical model for flow under both steady and transient conditions. The model is then used to examine the effect of uncertainty in boundary conditions and the effect of heterogeneity on the pressure head and flux variance profiles at various times for one-dimensional vertical flow cases. Dependence of pressure head variance on the flow conditions (drying or wetting) is examined. On the basis of the analysis it is found that the propagation of the head variance is similar to that of the concentration variance for solute transport in saturated aquifers. The head variance is proportional to the mean pressure gradient, and thus large head variances are associated with the wetting and the drying front of a moisture pulse. The peak head variance is smaller at the wetting front than it is at the drying front. This difference is attributed to the difference in the magnitude of mean hydraulic gradient and should not necessarily be interpreted as a hysteresis effect. In addition, it is shown how the variance of the flux of a moisture pulse increases with depth.

1. Introduction

Movement of water and pollutants in the vadose zone affects the growth of vegetation and wildlife, the amount of recharge and evapotranspiration, and overall water quality in every part of the world. Spatial variability of hydraulic properties in the vadose zone is one important factor that controls the migration rate and path of water and pollutants. Because of our incomplete knowledge about the spatial distribution of hydraulic properties, prediction of flow and transport processes in the vadose zone always involves some degree of uncertainty. To address the uncertainty, stochastic modeling of flow and solute transport processes becomes necessary [*Yeh*, 1992, 1998].

In the past two decades, stochastic approaches have been applied to analyze flow and solute transport in the vadose zone. *Dagan and Bresler* [1983] presented a solution for the problem of infiltration and redistribution in the unsaturated zone, visualized as a collection of vertically homogeneous columns with random saturated conductivity values. By employing an analytical first-order approach, *Yeh et al*. [1985a, b, c] analyzed the effect of multidimensional variability in saturated hydraulic conductivity and the pore size distribution parameter on unsaturated flow. They considered steady infiltration in unbounded domains under unit mean gradient conditions and developed a moisture dependent anisotropy concept. In addition, they found the spatial variability of the soil water pressure increases as soil becomes less saturated. *Mantoglou and Gelhar* [1987a, b] extended the analysis by *Yeh et al*. [1985a, b, c] to transient flow conditions in unbounded domains and found significant hysteresis in pressure head variance, unsaturated hydraulic conductivity, and moisture capacity. Although their results are interesting, they are limited to asymptotic behaviors because of limitations in the analytical method. *Protopapas and Bras* [1990] developed a numerical method to investigate uncertainty propagation with numerical models for flow and transport in the unsaturated zone. *Indelman et al*. [1993] used a perturbation analysis to investigate the unsaturated steady state flow through bounded heterogeneous formations. Few theoretical studies have focused on the effect of heterogeneity on unsaturated flow under transient conditions in bounded domains.

In this paper we develop a first-order stochastic model to examine the effect of uncertainty in both boundary conditions and heterogeneity on the propagation of pressure head and flux variances under transient flow conditions.

Paper number 1999WR900005.
0043-1397/99/1999WR900005$09.00

2. Mathematical Formulations

Strictly speaking, water movement in the vadose zone is directly associated with the movement of air. A rigorous analysis of water flow in the vadose zone should consider the flow of water and air. However, in many cases the movement of air can be ignored and Richards' equation is generally used:

$$\frac{\partial}{\partial x_i}\left(K_{ij}(h)\,\frac{\partial(h-x_1)}{\partial x_j}\right)=\frac{\partial\theta}{\partial t}+\varepsilon S_s\,\frac{\partial h}{\partial t}=(C(h)+\varepsilon S_s)\,\frac{\partial h}{\partial t} \tag{1}$$

where x_i and x_j are the spatial coordinates ($i, j = 1, 2$, and 3), x_1 corresponds to the vertical direction (positive downward), and $K_{ij}(h)$ is the hydraulic conductivity tensor which is a function of the soil-water pressure head, h. The pressure head is positive if the porous medium is fully saturated and it is negative when the medium is unsaturated. The moisture capacity term, $C(h)$, represents the amount of change in moisture content (θ) per unit change in negative pressure when the geological medium is partially saturated. It corresponds to the slope of the water release curve or moisture-pressure head relationship, $\theta(h)$, of a given soil. When the soil is fully saturated, the change in water storage due to change in the positive pressure is denoted by the specific storage term, S_s, which is related to the compressibility of the porous medium and water. In (1), ε is a saturation index of the porous medium: It is zero when the medium is unsaturated and is equal to one if the medium is fully saturated. Although this saturation index approach appears logical, it has seldom been tested. In our following analysis we will focus on the cases where the entire porous media are under fully unsaturated conditions, and therefore the effect of S_s is omitted.

2.1. First-Order Approximation of Head Variances

If Richards' equation is approximated by a fully implicit finite element scheme, it can be expressed in a matrix form as

$$\mathbf{P}(\mathbf{h_k}, \mathbf{p})\mathbf{h_k} = \mathbf{Q}(\mathbf{h_k}, \mathbf{p})\mathbf{h_{k-1}} + \mathbf{f}(\mathbf{h_k}, \mathbf{p}, \mathbf{u}) \tag{2}$$

Throughout this paper, boldface capital letters indicate matrices and boldface lowercase letters indicate vectors. In (2), $\mathbf{h_k}$ is the n-dimensional vector of the soil-water pressure head at the time t_k at each of the n nodes, where the subscript k denotes the time level; $\mathbf{p}$ is the $m \cdot n-$dimensional vector of the m parameters used to define the soil hydraulic properties; $\mathbf{u}$ is the boundary condition l-dimensional vector, where l is the number of boundary nodes ($l = 2$ for the one-dimensional case); $\mathbf{P}$ is the matrix associated with weighted unsaturated hydraulic conductivity values and moisture capacity terms evaluated at $\mathbf{h_k}$; $\mathbf{Q}$ is the matrix associated with the weighted moisture capacity term evaluated at $\mathbf{h_k}$; and the vector $\mathbf{f}$ is related to the boundary conditions and the gravity term. In this formulation we apply a linear shape-function to the mixed form of Richards' equation. That is, the moisture content is linearly weighted over the element; the rate of change in θ is related to the product of the moisture capacity term and the rate of change in h. As a result, the error in the mass balance is always less than 1% and the solution converges rapidly [*Bao*, 1995].

Using the Vetter "calculus" [*Dettinger and Wilson*, 1981; *Vetter*, 1970, 1971, 1973], expanding (1) in Taylor series around the mean, retaining terms up to the first order, and taking the expected value yield the approximate mean equation

$$\mathbf{P}(\langle\mathbf{h_k}\rangle, \langle\mathbf{p}\rangle)\langle\mathbf{h_k}\rangle = \mathbf{Q}(\langle\mathbf{h_k}\rangle, \langle\mathbf{p}\rangle)\langle\mathbf{h_{k-1}}\rangle + \mathbf{f}(\langle\mathbf{h_k}\rangle, \langle\mathbf{p}\rangle, \langle\mathbf{u}\rangle) \tag{3}$$

where the expectation is denoted by angle brackets. Equation (3) has the same form as (2), with the exception that the mean values of the parameters are used to derive the ensemble mean of the variables [*Dettinger and Wilson*, 1981].

Subtracting (3) from the Taylor expansion results in a perturbation equation

$$\mathbf{h'_k} = \mathbf{F_k}\mathbf{h'_{k-1}} + \mathbf{G_k}\mathbf{p'} + \mathbf{O_k}\mathbf{u'} \tag{4}$$

with

$$\begin{aligned}
\mathbf{E_k} &= (\mathbf{D_{h_k}P})(\mathbf{I_n}*\langle\mathbf{h_k}\rangle) + \mathbf{P}(\mathbf{D_{h_k}Q})(\mathbf{I_n}*\langle\mathbf{h_{k-1}}\rangle) - \mathbf{D_{h_k}f} \\
\mathbf{F_k} &= \mathbf{E_k^{-1}}[-\mathbf{Q}] \\
\mathbf{G_k} &= \mathbf{E_k^{-1}}[-(\mathbf{D_pP})(\mathbf{I_n}*\langle\mathbf{h_k}\rangle) + (\mathbf{D_pQ})(\mathbf{I_n}*\langle\mathbf{h_{k-1}}\rangle) + \mathbf{D_pf}] \\
\mathbf{O_k} &= \mathbf{E_k^{-1}}[(\mathbf{D_uf})]
\end{aligned} \tag{5}$$

where primes denote the perturbations. In (5), $\mathbf{D_xA}$ is the derivative of the matrix $\mathbf{A}$ with respect to the transpose of the vector $\mathbf{x}$. $\mathbf{I_n}$ is an $n \cdot n-$dimensional identity matrix, and the operator asterisk signifies the Kronecker product [*Dettinger and Wilson*, 1981]. Using a recursive formulation [*Protopapas and Bras*, 1990; *Townley and Wilson*, 1985], (4) can be written as

$$\mathbf{h'_k} = \mathbf{A_k}\mathbf{h'_0} + \mathbf{B_k}\mathbf{p'} + \mathbf{C_k}\mathbf{u'} \tag{6}$$

with

$$\begin{aligned}
\mathbf{A_k} &= \mathbf{F_k}\mathbf{A_{k-1}} \\
\mathbf{B_k} &= \mathbf{F_k}\mathbf{B_{k-1}} + \mathbf{G_k} \\
\mathbf{C_k} &= \mathbf{F_k}\mathbf{C_{k-1}} + \mathbf{O_k}
\end{aligned} \tag{7}$$

where $\mathbf{h'_0}$ represents the uncertainty in the initial condition. Similarly, the approximate mean equation for unsaturated flow under steady state conditions can be written as

$$\mathbf{S}(\langle\mathbf{h_s}\rangle, \langle\mathbf{p}\rangle)\langle\mathbf{h_s}\rangle = \mathbf{f}(\langle\mathbf{h_s}\rangle, \langle\mathbf{p}\rangle, \langle\mathbf{u}\rangle) \tag{8}$$

where the matrix $\mathbf{S}$ is similar to the matrix $\mathbf{P}$ but without the moisture capacity term. The perturbation equation is given as

$$\mathbf{h'_s} = \mathbf{G_0}\mathbf{p'} + \mathbf{O_0}\mathbf{u'} \tag{9}$$

where

$$\begin{aligned}
\mathbf{E_0} &= (\mathbf{D_{h_s}S})(\mathbf{I_n}*\mathbf{h_s}) + \mathbf{S} - \mathbf{D_{h_s}f} \\
\mathbf{G_0} &= \mathbf{E_0^{-1}}[-(\mathbf{D_pS})(\mathbf{I_n}*\mathbf{h_s}) + \mathbf{D_pf}] \\
\mathbf{O_0} &= \mathbf{E_0^{-1}}[(\mathbf{D_uf})]
\end{aligned} \tag{10}$$

Substituting this expression in equation (6), the $\mathbf{h'_k}$ perturbation at any given time becomes

$$\mathbf{h'_k} = \mathbf{B_k}\mathbf{p'} + \mathbf{C_k}\mathbf{u'} \tag{11}$$

with

$$\begin{aligned}
\mathbf{B_k} &= \mathbf{F_k}\mathbf{B_{k-1}} + \mathbf{G_k} \\
\mathbf{C_k} &= \mathbf{F_k}\mathbf{C_{k-1}} + \mathbf{O_k}
\end{aligned} \tag{12}$$

and

$$\mathbf{B_0} = \mathbf{G_0} \qquad \mathbf{C_0} = \mathbf{O_0} \tag{13}$$

By using (13), the relationship between the head covariance matrix $\mathbf{R_{hh}}$ and the parameter and boundary condition covariance matrices, $\mathbf{R_{pp}}$ and $\mathbf{R_{uu}}$, respectively, can be defined as

$$\mathbf{R_{hh}} = \langle\mathbf{h'_k}\mathbf{h'^T_k}\rangle = \mathbf{B_k}\mathbf{R_{pp}}\mathbf{B_k^T} + \mathbf{C_k}\mathbf{R_{uu}}\mathbf{C_k^T} \tag{14}$$

if the soil parameters and the boundary conditions are uncorrelated. The cross-covariance matrices between the head, parameters, and the boundary conditions are given by

$$\begin{aligned}
\mathbf{R_{hp}} &= \langle\mathbf{h'_k}\mathbf{p'^T}\rangle = \mathbf{B_k}\langle\mathbf{p'}\mathbf{p'^T}\rangle + \mathbf{C_k}\langle\mathbf{u'}\mathbf{p'^T}\rangle \\
&= \mathbf{B_k}\mathbf{R_{pp}} \\
\mathbf{R_{ph}} &= \mathbf{R_{hp}^T}
\end{aligned} \tag{15}$$

and

$$\mathbf{R_{hu}} = \langle \mathbf{h'_k u'^T} \rangle = \mathbf{G_k} \langle \mathbf{p' u'^T} \rangle + \mathbf{O_k} \langle \mathbf{u' p'^T} \rangle$$
$$= \mathbf{O_k R_{uu}} \qquad (16)$$
$$\mathbf{R_{uh}} = \mathbf{R_{hu}^T}$$

In the one-dimensional case, $\mathbf{R_{uu}}$ is a two-by-two matrix with the variance of boundary condition on the diagonal and zero on the off-diagonal terms.

For mathematical simplicity and for comparing with the results by *Mantoglou and Gelhar* [1987a, b], we chose *Gardner*'s [1958] model for describing the unsaturated hydraulic properties of soils in this study, although the presented numerical approach is not limited to this model. The model is given as

$$\log K(h) = \log K_s + \alpha h$$
$$\theta(h) = (\theta_s - \theta_r) * \exp(\alpha h) + \theta_r \qquad (17)$$
$$C(h) = (\theta_s - \theta_r) * \alpha \exp(\alpha h)$$

where log denotes the natural logarithm, K_s is the saturated hydraulic conductivity, α is the pore-size distribution parameter, θ_s is the saturated water content, and θ_r is the residual water content. For convenience, we will use f to denote $\log K_s$. If we consider α, f, θ_r, and θ_s as stochastic processes, then

$$\mathbf{R_{pp}} = \begin{bmatrix} \mathbf{R_{ff}} & \mathbf{R_{f\alpha}} & \mathbf{R_{f\theta_s}} & \mathbf{R_{f\theta_r}} \\ \mathbf{R_{\alpha f}} & \mathbf{R_{\alpha\alpha}} & \mathbf{R_{\alpha\theta_s}} & \mathbf{R_{\alpha\theta_r}} \\ \mathbf{R_{\theta_s f}} & \mathbf{R_{\theta_s\alpha}} & \mathbf{R_{\theta_s\theta_s}} & \mathbf{R_{\theta_s\theta_r}} \\ \mathbf{R_{\theta_r f}} & \mathbf{R_{\theta_r\alpha}} & \mathbf{R_{\theta_r\theta_s}} & \mathbf{R_{\theta_r\theta_r}} \end{bmatrix} \qquad (18)$$

where $\mathbf{R_{xy}}$ is the cross-covariance matrix of x and y. If x and y are uncorrelated, $\mathbf{R_{xy}}$ is zero. Otherwise, it must be specified.

2.2. First-Order Approximation of Flux Variance

The finite element formulation of Darcy's equation for the unsaturated flow yields

$$\mathbf{q} = \mathbf{t}(\mathbf{h_k}, \mathbf{p}, \mathbf{u}) \qquad (19)$$

where the vector $\mathbf{t}$ depends on the pressure head gradient and on the weighted unsaturated hydraulic conductivity values. The Taylor series expansion up to the first order of (19) gives

$$\mathbf{q} = \mathbf{t}(\langle \mathbf{h_k} \rangle, \langle \mathbf{p} \rangle, \langle \mathbf{u} \rangle) + (\mathbf{D_{h_k} t})(\mathbf{h_k} - \langle \mathbf{h_k} \rangle) + (\mathbf{D_p t})(\mathbf{p} - \langle \mathbf{p} \rangle)$$
$$+ (\mathbf{D_u t})(\mathbf{u} - \langle \mathbf{u} \rangle) \qquad (20)$$

The expected value of the flux is given by

$$\langle \mathbf{q} \rangle = \mathbf{t}(\langle \mathbf{h_k} \rangle, \langle \mathbf{p} \rangle, \langle \mathbf{u} \rangle) \qquad (21)$$

Therefore the perturbation equation is

$$\mathbf{q'} = \mathbf{M_{h_k} h'_k} + \mathbf{M_p p'} + \mathbf{M_u u'} \qquad (22)$$

with

$$\mathbf{M_{hk}} = \mathbf{D_{h_k} t}, \ \mathbf{M_{pk}} = \mathbf{D_p t}, \ \mathbf{M_{uk}} = \mathbf{D_u t} \qquad (23)$$

or

$$\mathbf{q'} = \mathbf{V_k p'} + \mathbf{Z_k u'} \qquad (24)$$

with

$$\mathbf{V_k} = \mathbf{M_{hk} B_k} + \mathbf{M_{pk}}$$
$$\mathbf{Z_k} = \mathbf{M_{hk} C_k} + \mathbf{M_{uk}} \qquad (25)$$

Using this formula, the approximate autocovariance matrix for the flux is given as

$$\mathbf{R_{qq}} = \langle \mathbf{q' q'^T} \rangle = \mathbf{M_{h_k} R_{hh} M_{h_k}^T} + \mathbf{M_{h_k} R_{hp} M_p^T} + \mathbf{M_{h_k} R_{hu} M_u^T}$$
$$+ \mathbf{M_p R_{ph} M_{h_k}^T} + \mathbf{M_p R_{pp} M_p^T} + \mathbf{M_u R_{uh} M_{h_k}^T} + \mathbf{M_u R_{uu} M_u^T} \qquad (26)$$

3. Results and Discussion

The above formulations are valid for multidimensional flow in unsaturated porous media but our numerical examples are limited to one-dimension vertical infiltration problems (perfectly stratified soil with uniform boundary conditions). In spite of this limitation the results of this preliminary analysis will enhance our understanding of the general behavior of flow in the heterogeneous vadose zone.

3.1. Comparison With Monte Carlo Simulation Results

The first-order model was first tested against the results of Monte Carlo simulations for flow in a one-dimensional, vertical soil profile under transient wetting and drying conditions. In this test the total length of the one-dimensional simulation domain was 5000 cm and was divided into 250 elements, each with a length of 20 cm. Equation (17) was used to represent the constitute relation of the unsaturated hydraulic property for each element. Soil parameters f, α, θ_s, and θ_r for each element were considered as second-order stationary Gaussian processes with the means of K_s equal to 10 cm/min, of α equal to 0.1 cm^{-1}, and of θ_s and θ_r equal to 0.4 and 0.06, respectively. The variances of f, α, θ_s and θ_r were 0.1, 10^{-7} cm^{-2}, 0.001, and 0.001, respectively, and the corresponding coefficients of variation were 3.1×10^{-2}, 3.1×10^{-3}, 7.9×10^{-2}, and 5.3×10^{-2}, respectively. Cross correlation between different hydraulic parameters was assumed negligible as partially suggested by field data [*Russo and Bouton*, 1992] and by the fact that the cross correlation between parameters reduces the head variance [*Yeh*, 1989]. Exponential covariance functions with an integral scale of 160 cm were used to describe the spatial structure of f, α, θ_s, and θ_r. Flux boundary conditions were assigned at the top of the soil profile for the wetting and drying cases, and a constant head, $h_n = 0$ cm (representing the water table) was specified as the bottom boundary condition. Mean and variance of the initial head profile for the wetting case were assigned equal to those from the steady state solution for an infiltration event of a mean flux (q_a) of 0.002 cm/min with a variance (σ_q^2) equal to 10^{-7} cm^2/min^2. In the drying case, means and variances of the initial head profile were generated with a prescribed mean flux ($q_a = 0.006$ cm/min) and variances ($\sigma_q^2 = 10^{-7}$ cm^2/min^2). A sudden change in the mean flux was then imposed on the top boundary condition. The flux was increased from the initial mean value $q_a = 0.002$ cm/min to $q_b = 0.006$ cm/min for the wetting case. It was decreased from $q_a = 0.006$ cm/min to $q_b = 0.002$ cm/min for the drying case. The variances associated with these prescribed fluxes were kept the same as the one in the initial steady state case.

For the Monte Carlo simulations, each element was assigned a value of f, α, θ_s, and θ_r, using a random field generator [*Yeh*, 1989] with the specified means and covariance functions. These 250 elements, with different hydraulic parameters, represent a possible heterogeneous soil profile. For each heterogeneous soil profile the fluxes at the top, q_a and q_b, were randomly

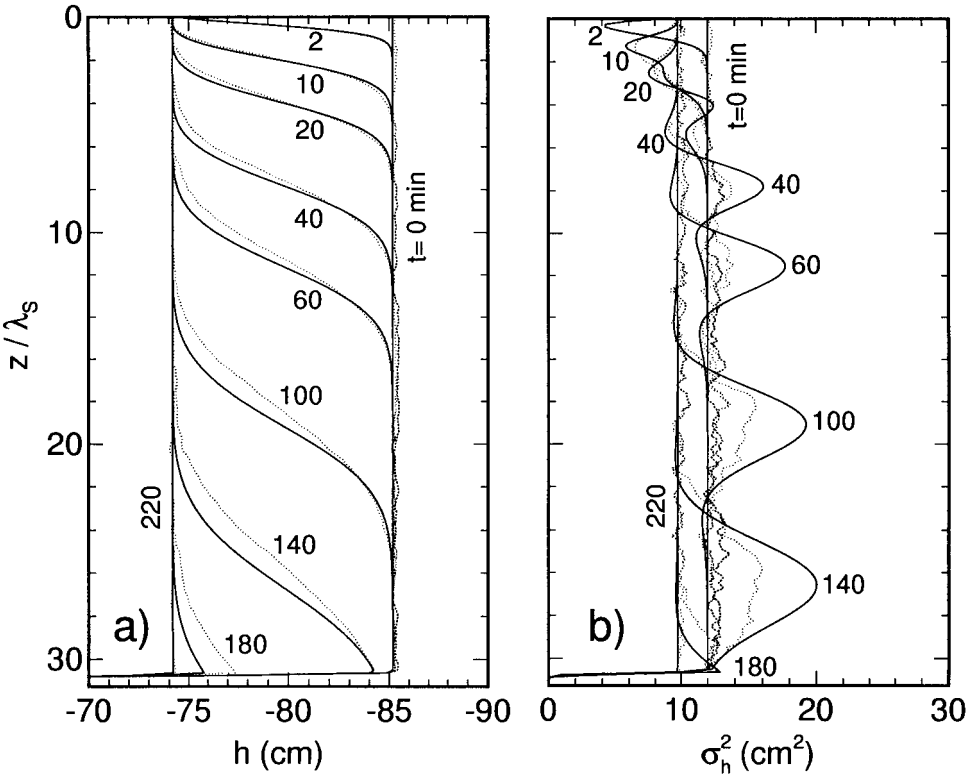

Figure 1. (a) The mean pressure head distributions and (b) the associated pressure head variances from the Monte Carlo simulations (dotted lines) and the first-order numerical model (solid lines) for the wetting case.

produced from a normal distribution with the previously defined means and variances. The bottom boundary condition was always kept as a constant head, $h_n = 0$ cm. Our mass conservative, finite element, unsaturated flow model, (2), was then used to derive the corresponding pressure head profiles at different times. Two thousand Monte Carlo simulations were conducted and the resultant head distributions were then averaged to obtain the mean head profile and its variance distribution at various times.

Figure 1a shows the mean head distributions during wetting derived from both the Monte Carlo simulations (dotted lines) and from the first-order numerical model (equation (3), solid lines) at various times (0, 2, 10, 40, 60, 100, 140, 180, and 220 min). Similarly, Figure 2a depicts the mean head distributions for the drying scenario. In this figure (as well as in Figures 4 and 5) depths are normalized with respect to the correlation scale λ_s. The variances associated with these mean head distributions are illustrated in Figures 1b and 2b for the wetting and the drying case, respectively. Since the numerical solution of the mean flow equation is first-order, some differences between the results from the Monte Carlo simulations and the numerical solutions are expected.

To explain the differences, consider the exact mean flow equation

$$\frac{\partial}{\partial z}\left[\langle K(h)\rangle\left(\frac{\partial\langle h\rangle}{\partial z}-1\right)\right]-\langle C(h)\rangle\frac{\partial\langle h\rangle}{\partial t}+\left\langle\frac{\partial}{\partial z}\left[K'(h)\left(\frac{\partial h'}{\partial z}\right)\right]-C'(h)\frac{\partial h'}{\partial t}\right\rangle=0 \quad (27)$$

The first two terms in (27) represent the effect of the mean unsaturated hydraulic conductivity, moisture capacity term, and mean head; the last two terms inside the expected value represent the effect of products of perturbations. Similarly, the exact mean flux boundary condition at the top can be written as

$$\langle q\rangle=-\langle K(h)\rangle\left(\frac{\partial\langle h\rangle}{\partial z}-1\right)+\left\langle K'(h)\left(\frac{\partial h'}{\partial z}\right)\right\rangle \quad (28)$$

The boundary condition at the water table is $\langle h\rangle$ and $h' = 0$. Under steady state flow conditions with the given mean flux, the exact governing mean flow equation is

$$\frac{\partial}{\partial z}\left[\langle K(h)\rangle\left(\frac{\partial\langle h\rangle}{\partial z}-1\right)\right]+\left\langle\frac{\partial}{\partial z}\left[K'(h)\left(\frac{\partial h'}{\partial z}\right)\right]\right\rangle=0 \quad (29)$$

Notice that this mean flow equation is different from the equation employed in the first-order analysis, which is

$$\frac{\partial}{\partial z}\left[\langle K(h)\rangle\left(\frac{\partial h}{\partial z}-1\right)\right]=0 \quad (30)$$

In (30) the product of perturbations in (29) is omitted, and the head solution, h, in (30) is therefore expected to be different from the mean head, $\langle h\rangle$. Similarly, our first-order numerical model for transient flow also neglects the two terms inside the expectation brackets in (27). Furthermore, we must also point it out that our numerical analysis assumes that $\langle K(h)\rangle$ and $\langle C(h)\rangle$ in (27) can be approximated by (17) using mean values of f and α. Because of these simplifications, the mean head distributions from the first-order approach are expected to be different from the ensemble mean head profiles derived from the Monte Carlo simulation. The difference in head variances between the Monte Carlo simulation and our numerical approach is also anticipated. These discrepancies, however, will be small if the perturbation is small (i.e., soils with mild het-

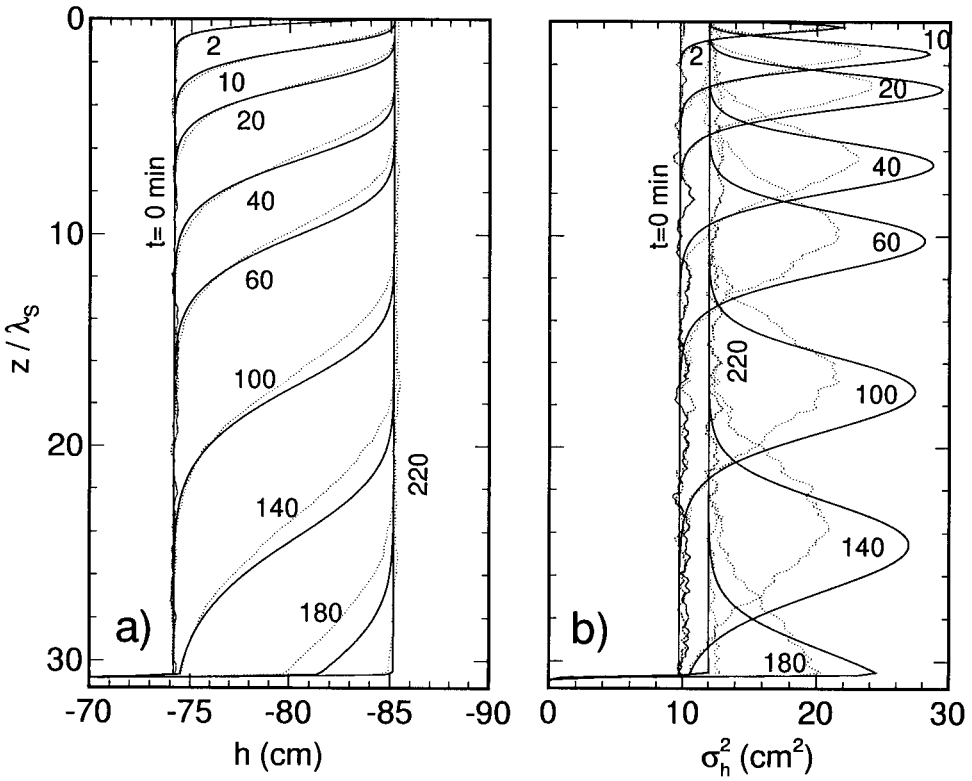

Figure 2. (a) The mean pressure head distributions and (b) the associated pressure head variances from the Monte Carlo simulations (dotted lines) and the first-order numerical model (solid lines) for the drying case.

erogeneity in unsaturated hydraulic conductivity). Notice that our first-order approximation is identical to the analytical spectral approach used by *Yeh et al*. [1985a, b] and *Mantoglou and Gelhar* [1987a, b], except that the analytical approach assumes that mean head is given.

We want to emphasize that the goal of this study is not to develop exact mathematical solutions to the stochastic Richards equation but to investigate the effect of heterogeneity on transient flow in unsaturated soils. Development of an exact solution to the stochastic flow equation is intractable even under the saturated flow conditions. For these reasons our test does not seek exact agreement in the values of mean and variance of pressure head between our approximation and the Monte Carlo solution. We rather focus on the general correspondence between the two solutions.

3.2. Behavior of Head Variance in Wetting and Drying Cases

Figures 1b and 2b show the propagation of head variances for the wetting and drying cases, respectively. In both cases the initial ($t = 0$ min) and final ($t = 220$ min) steady state head distributions are uniform for most of the depth (unit gradient condition), except near the water table. As expected, the head variances at $t = 0$ min and $t = 220$ min depend on the mean head value, in excellent agreement with the results from the spectral analysis assuming unit mean gradient [*Yeh et al*., 1985a, b; *Yeh*, 1989] if the variance of the boundary flux is omitted.

Transition from one steady state to the other takes place only at the wetting and drying fronts (Figure 1b). In a wetting scenario the head variances at locations where the wetting front has passed conform to final steady state head variance ($t = 220$ min), while the head variances at locations preceding the front remain equal to the steady state head variance at $t = 0$. Transient effects on the head variability are then exhibited at the wetting front location. Notice that during the early times ($t < 20$ min) head variances associated with the mean wetting front are less than the initial head variance. In addition, the minimum head variance approximately coincides with the inflection point of the mean wetting front, where the mean pressure head gradient is the greatest. Such behaviors are attributed to the effect of the prescribed flux boundary condition used in the simulation. After $t > 20$ min, the head variance at the inflection point of the wetting front gradually increases to its maximum. As the mean wetting front moves further downward, this head variance becomes even greater than the initial steady state head variance ($t = 0$). However, it rapidly decreases to the steady state solution once the front reaches the capillary fringe, where the conditioning effect of the water table boundary condition takes place.

In contrast to the wetting case, the head variances at the drying front are always greater than the initial steady state head variances (Figure 2b). The maximum value of the head variance follows the inflection point of the mean drying front where the mean pressure gradient is the greatest. It grows rapidly at the very early time and then decreases as the front moves downward. Once the front reaches the capillary fringe, the maximum head variance decreases toward the final steady state value. Figures 1b and 2b also show that the head variance at the drying front is greater than that at the wetting front.

The findings described above apply to both our first-order numerical model and the Monte Carlo simulation results. Therefore we conclude that our first-order approximate nu-

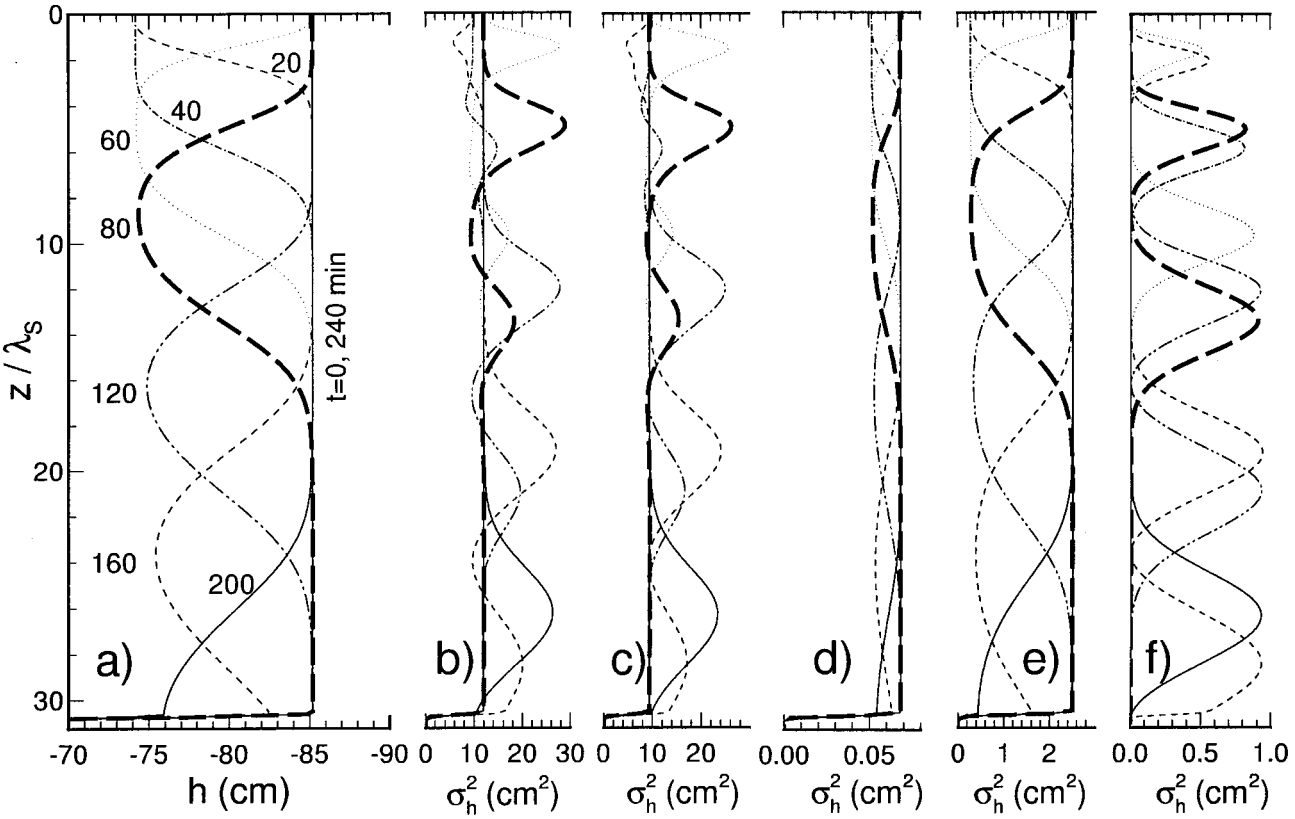

Figure 3. (a) The mean pressure head distributions, (b) the associated total pressure head variances, and the components due to the variability in (c) log K_s, (d) α, (e) q, and (f) θ_s or θ_r.

merical model is able to capture the general behavior of the "exact" solution to the stochastic differential equation. The following discussion will then focus on the behavior derived from our first-order approximation.

3.3. Impacts of Uncertainties of Input Parameters on Head Variances

Since our numerical uncertainty model is linear with respect to parameter variances and soil parameters are uncorrelated, analysis of the individual contribution of the uncertainties in f, α, the flux at the land surface (q), and θ_s and θ_r to the head variance becomes possible. To do so, the soil properties, initial conditions and boundary conditions were kept the same as the previous wetting case but q_b was reduced to q_a after 40 min. Thus a moisture pulse propagating toward the water table is created. Figure 3a shows the propagation of the corresponding mean pressure head pulse along the soil profile. As expected, as the pulse moves toward the water table, the peak of the mean pressure pulse decreases; the wetting and drying limbs of the pulse broaden because of the diffusive nature of the process. Notice that the drying front is always steeper than the wetting front. This is attributed to the fact that the drying front lags behind the wetting front and has less time for diffusion than the wetting front.

Propagation of the total pressure head variance (due to uncertainty in f, α, q, θ_s, and θ_r) associated with the mean head pulse as a function of time is shown in Figure 3b. In general, two peak head variances were observed: one associated with the wetting limb and the other with the drying limb. This result is similar to the concentration variance distribution of a mean concentration plume [*Sudicky*, 1986]. At early times ($t \leq 20$ min) the head variance associated with the wetting front is small because of the boundary. Since then, the head variance grows and becomes greater than the initial head variance. The peak variance of the wetting front also grows as the front moves toward the water table, but it starts to diminish when the front reaches the capillary fringe. The peak variance of the drying front, in contrast to that of the mean wetting limb, continuously decreases as the pulse moves toward the water table. In addition, the peak variance associated with the drying limb is always larger than that with the wetting limb. This result is different from the finding by *Mantoglou and Gelhar* [1987b] that the head variance is greater during the wetting than the drying.

Figure 3c shows the effect of variability in f on the head variance propagation. Impacts from the variability in α, q, and θ_s (or θ_r) are illustrated in Figures 3d, 3e, and 3f, respectively. Note that θ_s and θ_r are assumed to be independent from each other and the effects of uncertainty in θ_s and that in θ_r on head variance are essentially identical. According to Figures 3c and 3f, influences on the head variances caused by variability in the parameters, f, θ_s, or θ_r, are similar. They all are related to the magnitude of the mean pressure head gradient regardless of wetting or drying. Consequently, the profile of the head variance due to the variability in f shows two peaks: one associated with the maximum pressure head gradient at the wetting limb and the other at the drying limb. At locations where the mean pressure gradient is equal to zero (at the peak, in front of the wetting front, and behind the drying front), the head variance

due to the variability in f matches that of the steady state flow and is independent of the mean head. Similar behavior is also observed in Figure 3f, but the steady state head variance is zero (since the steady-state equation does not include θ_s and θ_r). Also, the impact of the variability in f on the head variance is found to be greater during drying than during wetting. On the other hand, the effects of the uncertainties in θ_s and θ_r on the peak head variances in the drying and the wetting limbs are almost identical.

The distribution of the head variance due to uncertainties in α and q (Figures 3d and 3e) resembles that of the mean pressure head pulse (Figure 3a). The contributions from the variability in α and q to the head variance are found to be related to the magnitude of the mean pressure head. In addition, they are bounded by the steady state results; that is, the variances in head at the peak of the mean pressure pulse (where the pressure gradient is zero) conform to the steady state solution for a unit mean hydraulic gradient as pointed out by *Mantoglou and Gelhar* [1987b].

Our simulation results also show that the peak of total head variance depends on the initial mean pressure head. That is, a given flux will produce greater mean pressure head gradients at both wetting and drying limbs of the pressure pulse in the initially dry soil than in the wet soil. Since the contributions from the variabilities in f, θ_s, and θ_r to the peak head variance explicitly depend upon the mean pressure head gradient, they thus increase with the dryness of the initial condition. On the other hand, the impacts of α and q on the peak head variance are proportional to the mean head value at the location where the maximum head gradient exists. The mean head value of the pressure pulse in the initially dry soil is larger than that in the wet soil. As a result, influences of α and q on the peak total variance increase if the soil is dry initially.

Possible hysteresis in head variance during transient infiltration as reported by *Mantoglou and Gelhar* [1987b] is also investigated for this case. *Mantoglou and Gelhar* [1987b] examined unsaturated infiltration into perfectly stratified random porous media under transient conditions. They found that the head variance was larger during wetting than during drying, and they attributed the difference to the hysteresis effect in the head variance. On the other hand, the results of our Monte Carlo simulation and the first-order numerical model showed that the head variance was smaller during wetting than during drying. More importantly, the difference in head variance during wetting and drying appears to be related to the difference in mean pressure gradient. Note that the flow field in their analysis is identical to ours (i.e., a one-dimensional flow phenomenon) because of uniform mean flow and perfect stratification assumption. Such possible dependence of peak head variance on the magnitude (i.e., absolute value) of pressure gradient leads us to ponder the hysteresis interpretation of *Mantoglou and Gelhar* [1987b].

Hysteresis has generally been observed in unsaturated hydraulic conductivity and moisture release data measured in the laboratory [*Klute*, 1986]. Most of these measurements of unsaturated hydraulic conductivity are determined by using the unit-gradient approach under steady state conditions. This unit-gradient approach implies that the hysteresis effect in the unsaturated hydraulic conductivity is independent of the hydraulic gradient. That is, if values of the mean hydraulic gradient and pressure during wetting and drying are the same, differences in hydraulic conductivity during wetting and drying can then be interpreted as a hysteresis effect. For the same token, the hysteretic behavior in head variances must be independent of the hydraulic gradient.

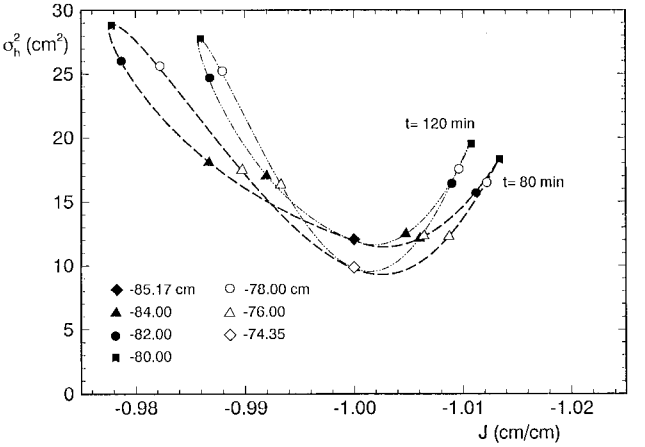

Figure 4. Dependence of σ_h^2 on mean hydraulic gradient and on mean pressure head, for the pressure head pulse of Figure 3 at two different times.

To explore the dependence of the head variance on the mean hydraulic gradient in this study, head variances are examined at every location of the moisture pulses in Figure 3 at two time levels ($t = 80$ and 120 min). These head variances are plotted in Figure 4 as a function of the corresponding mean hydraulic gradient ($J = d\langle h\rangle/dz - 1$). The long dashed line denotes head variances along the moisture pulse at $t = 80$ min (see Figure 3), whereas the dotted-dashed line represents those at $t = 120$ min. To facilitate a comparison with the result of *Mantoglou and Gelhar* [1987b], the effect of the variance in the flux boundary condition is not considered in the case. As illustrated in this figure, the head variance is directly related to the mean hydraulic gradient in a complex fashion, and it partially depends on the mean pressure head. Notice that for both moisture pluses, two head variances (the open and solid diamonds) exist when the mean hydraulic gradient equals the unity ($J = -1$). The open diamond represents the variance of head at the peak of the moisture pulse, while the solid diamond denotes the variances in front of and behind the moisture pulse, corresponding to that of the initial steady state condition. Because the soil was initially dry and then wetted by the moisture pulse, the open diamond has a lower value in head variance than the solid one. As one moves away from the peak of the moisture pulse towards the wetting front, the magnitude of mean hydraulic gradient increases and reaches a maximum at the inflection point of the wetting front (i.e., from $J = -1.00$ to $J - 1.012$). The head variance first slightly decreases and increases accordingly to a maximum. After this maximum at the wetting front, the head variance decreases because of the decrease in the mean hydraulic gradient. Finally it reaches the value of the head variance corresponding to the initial steady-state condition (the solid diamond). The behavior of head variances along the drying limb of the moisture pulse is also influenced by the mean hydraulic gradient and can be similarly depicted. However, the magnitude of mean hydraulic gradient is less than 1 at the drying limb since the pressure head gradient is positive.

To isolate the effect of the mean pressure head on the variance in Figure 4, the head variances corresponding to the same mean pressure head values along the wetting and drying

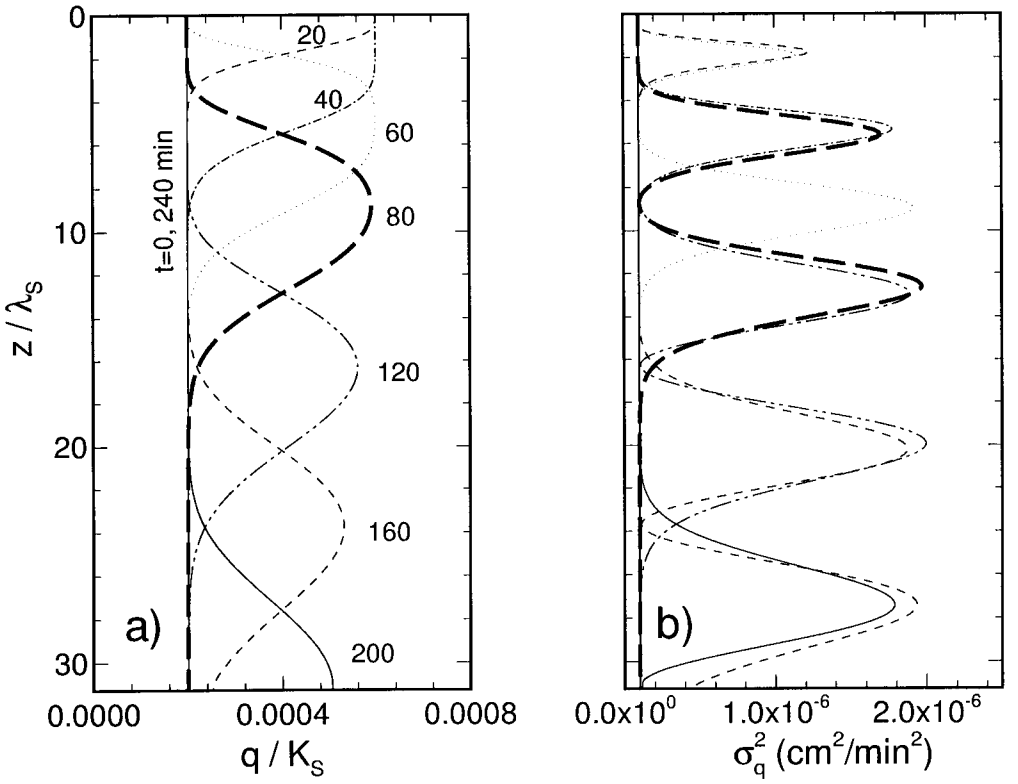

Figure 5. (a) The mean flux distributions and (b) the associated flux variances for the pressure head pulse of Figure 3.

limbs of the two moisture pulses are denoted using the same symbol. For example, the two solid circles for the pulse at t = 80 min represent the head variances at two locations in the wetting and drying fronts where the mean pressure head values are −76.0 cm. At this mean pressure head, the head variance (15.5 cm^2) at the wetting limb is found smaller than that (26.1 cm^2) at the drying limb. Therefore the difference in the head variances at this mean pressure head can then be attributed solely to the difference in the mean hydraulic gradients (i.e., −1.011 and −0.979). This is also true for the other head variances. The analysis of the Monte Carlo simulation for the case in Figure 3 also confirms the general dependence of the head variance on J and mean pressure head.

An explicit relationship between the head variances and both the mean hydraulic gradient and the mean head value is difficult to derive from this numerical result. Nevertheless, our qualitative finding suggests that the greater variance during drying than wetting may be related to the mean hydraulic gradient. As a result, hysteresis in head variance suggested by *Mantoglou and Gelhar* [1987b] may not exist during transient unsaturated flow in the hypothetical soil with perfect stratification. In fact, results of stochastic analysis of steady state infiltration in heterogeneous soils by *Yeh et al*. [1985a, b, c] also suggest nonhysteresis behavior in head variances and effective hydraulic conductivity. The nonhysteresis behavior may be attributed to the fact that the hysteresis in hydraulic properties of the soil at the local scale is ignored in the analysis.

3.4. Flux Variance

The means and variances of the flux associated with the pulse at different time levels, evaluated using (21) and (26), are illustrated in Figure 5. Since the flow is one-dimensional and steady and the mean flux is constant over the depth before and behind the pulse, the flux variances at these locations are equal to the flux variance specified at the boundary. Over the moisture pulse the distribution of the flux variance has two peaks similar to the head variance distribution in Figure 3. The peak variances in flux at the wetting and drying fronts are found to be related to the gradient of the mean flux. However, they grow as the fronts move toward the water table and without being affected by the water table boundary condition. This growth in the flux variance may suggest that our recharge estimate in thick stratified vadose zones is subject to greater uncertainty due to heterogeneity. Although evapotranspiration is not considered in our study, it may further amplify the uncertainty in the estimate of recharge. More importantly, this result is different from those derived from analysis that assumes that the vadose zone consists of a bundle of vertical stream tubes [*Dagan and Bresler*, 1983]. The variance of flux based on the vertical stream tube model will remain the same as that specified at the top boundary as the moisture pulse propagates downward. Our approach however indicates that uncertainty in flux increases as the moisture pulse moves downward since it encounters more heterogeneity. This result seems logical and indicates that the vertical stream tube model may not be suitable for most field situations where vertical stratification is significant.

4. Conclusions

A first-order numerical model for the stochastic analysis of transient flow through unsaturated soils is developed. This

model can be used to investigate the effect of heterogeneity on flow under realistic conditions, such as bounded domains, uncertainty in boundary and initial conditions, and nonstationary processes. More importantly, it allows us to examine many cases excluded by previously developed analytical methods [e.g., *Mantoglou and Gelhar*, 1987a, b]. The model has been verified against the results of Monte Carlo simulations. Overall, the evolution of the head and flux variances derived from the numerical model is in good agreement with that obtained from the Monte Carlo simulations.

On the basis of our analysis, we found that the overall behavior of the head variances produced by the variability in f, θ_s, and θ_r is different from that produced by the variability in α and in the prescribed flux q. Similar to the propagation of the concentration variance in saturated aquifers, the head and flux variances are strongly correlated to the mean hydraulic gradient at the inflection point of the wetting or drying front. Our finding does not support the hysteresis behavior in head variance reported by *Mantoglou and Gelhar* [1987b]. This finding, more importantly, leads us to question the mechanisms of hysteresis in effective properties for large-scale vadose zones.

We found that while the mean flux remains the same throughout the entire vadose zone, the variance of flux grows with depth towards the water table. This result implies that our estimate of the recharge in a thick stratified vadose zone may be greatly uncertain.

Finally, we want to point out that our analysis is based on a one-dimensional model. The variances in head and flux are expected to be greater than those derived from a three-dimensional model. Nevertheless, the general relationship between the input and output variances in a one-dimensional model is similar to those in a three-dimensional analysis [*Yeh et al*., 1985a, b, c].

Although the Gardner's model, (17), for unsaturated hydraulic properties may not be representative for all soils, no universal unsaturated hydraulic property model exists. Previous studies [*Yeh et al*., 1985a, b, c; *Hopman et al*., 1988; *Unlu et al*., 1990] have shown that the general behavior of flow observed in the vadose zone is adequately described by Gardner's model. Results of a recent analysis by *Zhang et al*. [1998] seem to validate this hypothesis.

Acknowledgments. The study is partially supported by NSF (grant EAR 9317009) and CNR Strategic Project "Drinking Water Scarcity Management." The work was carried out while the first author was a visiting scholar in the Department of Hydrology and Water Resources at The University of Arizona, Tucson, in 1996. Supports from L. Ubertini and G. Margaritora are acknowledged.

References

Bao, X., Mesh design for numerical solution of Richards' equation, M.S. thesis, Dep. of Hydrol. and Water Resour., Univ. of Ariz., Tucson, 1995.

Dagan, G., and E. Bresler, Unsaturated flow in spatially variable fields, 1, Derivation of models of infiltration and redistribution, *Water Resour. Res*., *19*(2), 413–420, 1983.

Dettinger, M. D., and J. L. Wilson, First order analysis of uncertainty in numerical models of groundwater flow, 1, Mathematical development, *Water Resour. Res*., *17*(1), 149–161, 1981.

Gardner, W. R., Some steady-state solutions of unsaturated moisture flow equations with application to evaporation from a water table, *Soil Sci*., *85*, 228–232, 1958.

Hopman, J. W., H. Schukking, and P. J. J. F. Torfs, Two-dimensional steady state unsaturated water flow in heterogeneous soils with autocorrelated soil hydraulic properties, *Water Resour. Res*., *24*(12), 2005–2017, 1988.

Indelman, P., D. Or, and Y. Rubin, Stochastic analysis of unsaturated steady state flow through bounded heterogeneous formations, *Water Resour. Res*., *29*(4), 1141–1148, 1993.

Klute, A. (Ed.), *Methods of Soil Analysis*, 1186 pp., Soil Sci. Soc. of Am., Madison, Wis., 1986.

Mantoglou, A., and L. W. Gelhar, Capillary tension head variance, mean soil moisture content, and effective specific soil moisture capacity of transient unsaturated flow in stratified soils, *Water Resour. Res*., *23*(1), 47–56, 1987a.

Mantoglou, A., and L. W. Gelhar, Effective hydraulic conductivities for transient unsaturated flow in stratified soils, *Water Resour. Res*., *23*(1), 57–67, 1987b.

Protopapas, A. L., and R. L. Bras, Uncertainty propagation with numerical models for flow and transport in the unsaturated zone, *Water Resour. Res*., *26*(10), 2463–2474, 1990.

Russo, D., and M. Bouton, Statistical analysis of spatial variability in unsaturated flow parameters, *Water Resour. Res*., *28*(7), 1911–1925, 1992.

Sudicky, E. A., A natural gradient experiment on solute transport in a sand aquifer: Spatial variability of hydraulic conductivity and its role in the dispersion process, *Water Resour. Res*., *22*(2), 2069–2082, 1986.

Townley, L. R., and J. L. Wilson, Computationally efficient algorithms for parameter estimation and uncertainty propagation in numerical models of groundwater flow, *Water Resour. Res*., *21*(12), 1851–1860, 1985.

Unlu, J., D. R. Nielsen, and J. W. Biggar, Stochastic analysis of unsaturated flow: One-dimensional Monte Carlo simulations and comparison with spectral perturbation analysis and field observations, *Water Resour. Res*., *26*(9), 2207–2218, 1990.

Vetter, W. J., Derivative operations on matrices, *IEE Trans. Autom. Control*, *15*, 241–244, 1970.

Vetter, W. J., Correction to: Derivative operations on matrices, *IEE Trans. Autom. Control*, *16*, 113, 1971.

Vetter, W. J., Matrix calculus operations and Taylor expansions, *SIAM Rev*., *15*(2), 352–369, 1973.

Yeh, T.-C. J., One-dimensional steady-state infiltration in heterogeneous soils, *Water Resour. Res*., *25*(10), 2149–2158, 1989.

Yeh, T.-C. J., Stochastic modeling of groundwater flow and solute transport in aquifers, *Hydrol. Processes*, *6*, 369–395, 1992.

Yeh, T.-C. J., Scale issues of heterogeneity in vadose zone hydrology, in *Scale Dependence and Scale Invariance in Hydrology*, edited by G. Sposito, Cambridge Univ. Press, New York, 1998.

Yeh, T.-C. J., L. W. Gelhar, and A. L. Gutjahr, Stochastic analysis of unsaturated flow, 1, Heterogeneous soils, *Water Resour. Res*., *21*(4), 447–456, 1985a.

Yeh, T.-C. J., L. W. Gelhar, and A. L. Gutjahr, Stochastic analysis of unsaturated flow, 2, Statistically anysotropic media with variable α, *Water Resour. Res*., *21*(4), 457–464, 1985b.

Yeh, T.-C. J., L. W. Gelhar, and A. L. Gutjahr, Stochastic analysis of unsaturated flow, 3, Observation and applications, *Water Resour. Res*., *21*(4), 465–471, 1985c.

Zhang, D., T. C. Wallstrom, and C. L. Winter, Stochastic analysis of steady-state unsaturated flow in heterogeneous media: Comparison of the Brooks-Corey and Garnder-Russo models, *Water Resour. Res*., *34*(6), 1437–1450, 1998.

M. Ferrante, Istituto di Idraulica, Universita' degli Studi di Perugia, Via G. Duranti 93, Perugia 06125, Italy. (ferrante@unipg.it)

T.-C. J. Yeh, Department of Hydrology and Water Resources, University of Arizona, Tucson, AZ 85721.

(Received April 14, 1998; revised December 9, 1998;
accepted December 30, 1998.)